Fourth LACCEI International Latin American and Caribbean Conference for Engineering and Technology (LACCET'2006)
"Breaking Frontiers and Barriers in Engineering: Education, Research and Practice"
21-23 June 2006, Mayagüez, Puerto Rico

Effect of Change in Pole Shape Design on Harmonic Contents of PM Synchronous Motor Air Gap Flux Density Waveform

Osama Mohammed, PhD
Professor, Florida International University, Miami, FL, USA

S. Ganu, PhD student
Visiting Researcher, Florida International University, Miami, FL, USA

N. Abed, PhD Student
PhD student, Florida International University, Miami, FL, USA

Abstract
This paper utilizes the wavelet packet transform to study the effects of change in the shape of the magnetic pole on the harmonic behavior of air gap flux density waveform. A surface mounted PM motor is used as an example. The original design contains 6 PM poles and 36 stator slots. The rotor and the stator winding are redesigned to have 4, 8, and 12 poles. The air gap flux density waveform is obtained from the finite element solutions. The results have been compared with different pole structure design. It has been found that there is not much difference in the harmonic content due to change in PM pole structure on the air gap flux density waveform.

Keywords
PM synchronous motor, wavelet packet transform, winding change

1. Introduction

Conventional analytical design and analysis methods of AC machines follow the assumption of having sinusoidal flux waveform in the air gap. An increase in the number of poles can be utilized for increasing the machine power density or for satisfying the lower speed demands at some application fields. This reduces the number of slots per pole per phase which finally leads to the increase in the harmonics of air gap flux waveform [Mohammed et al., 2004].
Increase in the harmonics can cause a variety of undesirable effects in the energy system. For example, harmonics can cause signal interference, over voltages, and circuit breaker failure, as well as equipment overheating, malfunction, and failure. Harmonics can cause excessive heating in system components, resulting in shortened life or failure. Rotor heating and pulsating output torque caused by harmonics can result in excessive motor heating and inefficiency. In other words, the harmonic increase will affect both the machine performance and the machine control system performance.
Wavelet transform proves to have some advantages when compared to the classical FFT (Fast Fourier Transform)-based algorithms. Unlike FFT, the periodicity of the signal is not required and erroneous results are avoided using wavelet packets. The wavelet packet method solves this problem by decomposing the measurement signal into a family of time finite signals through a filter-bank resulting in

multi-scale wavelet decomposition. Harmonics of the fundamental frequency, sub-harmonics and inter-harmonics are considered, disregarding the length of their occurrence in time.
This paper is organized as follows. First the remodeling of the motors having different pole based on the original machine is given. It includes the rearranging of the winding in the slots and the PM poles on the rotor iron surface. FE computation is performed on these different designs to obtain the field distribution and the flux density waveform in the air gap. Then the wavelet and wavelet packet theory are briefly introduced. Their implementation on the air gap flux density waveform is presented next.

2. Design of Different Pole Numbers

The original surface mounted PM synchronous motor has 6 poles on the rotor iron and 36 slots in the stator iron. One pole of the motor is shown in figure 1. The winding is double layer and excited with 3 phase supply. Slots per pole per phase (spp) are 2 (36/3*6). The magnets are radially magnetized. Their operating point is B_r =1.08 Tesla and μ_r =1.07. The angular magnet pole width is 50 degrees mechanical. Nonlinear BH curves are used for both stator and rotor iron. In order to form different number of poles, the stator winding needs to be rearranged so as to form same number of poles on stator as that of rotor. Winding arrangement for different number of poles is shown in figure 2.

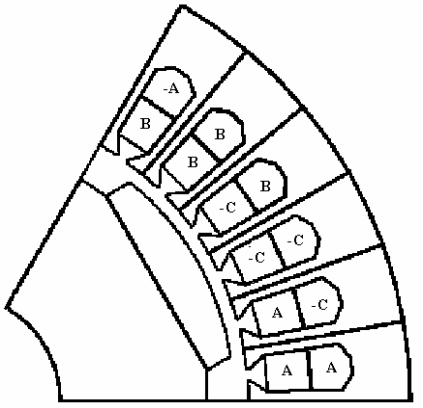

Figure 1: One pole of pm synchronous motor

4 POLE

A	A	A	-C	-C	-C	B	B	B	-A	-A	-A	C	C	C	-B	-B	-B
A	A	A	-C	-C	-C	B	B	B	-A	-A	-A	C	C	C	-B	-B	-B

6 POLE

A	A	-C	-C	B	B	-A	-A	C	C	-B	-B	A	A	-C	-C
A	A	-C	-C	B	B	-A	-A	C	C	-B	-B	A	A	-C	-C

8 POLE

A	A	-C	B	B	-A	C	C	-B	A	A	-C	B	B	-A	C
A	-C	-C	B	-A	-A	C	-B	-B	A	-C	-C	B	-A	-A	C

12 POLE

A	-C	B	-A	C	-B	A	-C	B	-A	C	-B	A	-C	B	-A
A	-C	B	-A	C	-B	A	-C	B	-A	C	-B	A	-C	B	-A

Figure 2: Winding arrangement in different pole designs up to 18 slots in all simulated machines

Depending on the number of poles, spp will change. As the number of poles goes on increasing, each phase will occupy less number of slots. The angular magnetic pole width is kept constant for all the pole variations. The air gap between permanent magnets gets adjusted accordingly. The dimensions of the stator yoke and stator teeth in all the topologies are kept unchanged. All radial and axial dimensions for motor are same in all the cases. Obviously, iron part in the motor having higher number of poles will be operating at higher flux density level and goes towards saturation. Saturation is one of the important factors causing harmonic increase in the air gap flux density waveforms along with slotting effects.

3. Finite Element Analysis (FEA)

Following formulation is used for solving the transient magnetic solution.

$$\sigma \frac{\partial \bar{A}}{\partial t} + \nabla \times \left(\nu \nabla \times \bar{A} \right) = \sigma \nabla V + \nabla \times \bar{H}_c \qquad (1)$$

Where, σ is electrical conductivity, $\bar{A}$ is magnetic vector potential, ν is reluctivity, V is electrical scalar potential, $\bar{H}_c$ is magnetic coercivity.

Nonlinear transient FE analysis was performed for the field calculation using commercial software of Flux2d. The transient analysis consists of electromagnetic field formulation and electric circuit formulation. Each formulation provides different matrices. These are coupled and solved simultaneously at every time solution. All field, circuit and motion equations are descritized in time domain. A converged solution is obtained at each time step. Moving air gap feature is utilized for the transient operation. The air gap is divided into 3 layers, one belonging to stator, one to the rotor and middle one which actually causes the rotor to move without changing the mesh. Rating of the motor is 2 hp, 3 phase, 1200 rpm, 6 pole, 60 Hz, 36 slots, 2inch deep, half slot current 128 Amp-turns. Half slot current is maintained constant throughout all pole arrangements. Considering motor periodicities, only quarter geometry is modeled for 4, 8, 12 poles while for 6 poles one sixth geometry is modeled. For all the simulation cases, different velocity is assigned to the rotor to adjust the angular frequency in the stator winding to be equal to 60 Hz. Speed is equal to 1800, 1200, 900 and 600 rpm in 4, 6, 8, 12 poles respectively. The rotor is rotated through every one degree with different time step depending upon the speed of the rotor to complete 360 degrees mechanical cycle. Flux density values are taken at the last instant. 2048 points were used in capturing the waveform in order to extract the frequencies up to 32 bands from wavelet analysis. Figure 3 shows field lines while figure 4 shows flux density waveform in air gap for different pole designs.

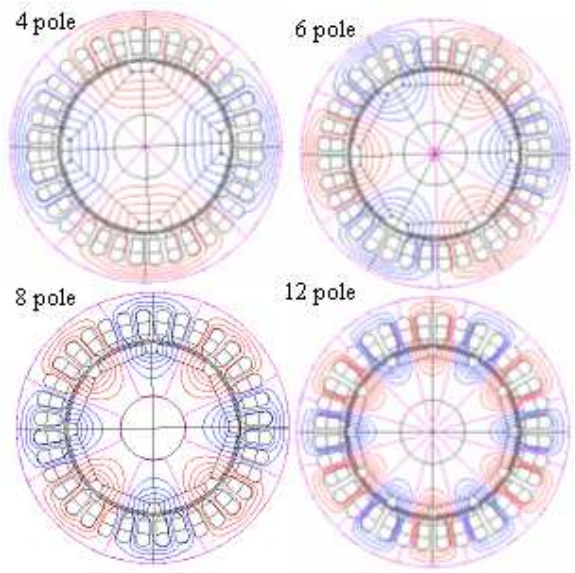

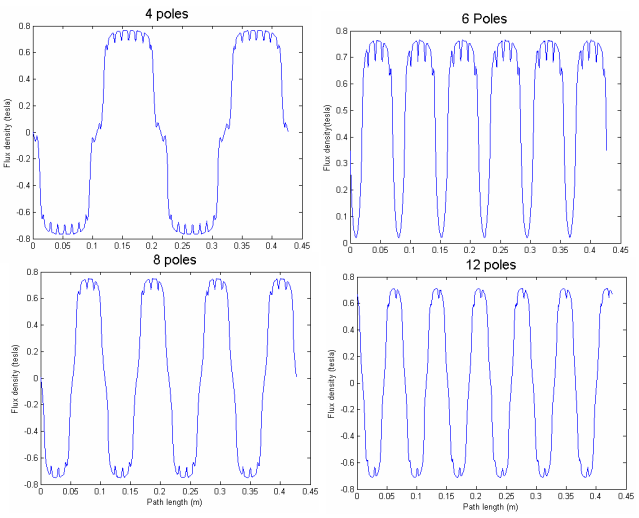

Figure 3: Field lines for different pole numbers **Figure 4: Flux density waveforms in air gap**

4. Wavelet Theory

4.1 Introduction

As in fourier transform(FT), the wavelet transform(WT) consists of decomposing a given function into a set of "building blocks". However, as opposed to the fourier transformation in which the "building blocks" are the well-known complex exponentials, the wavelet transform uses the dilated and translated version of a "mother wavelet" which has convenient properties according to time/frequency localization. Unlike FT which gives a global presentation of the signal, WT provides a local representation (in both time and frequency) of a signal; therefore it is suitable for analyzing a signal where time/frequency resolution is needed.

4.2 Multiresolution analysis

A multiresolution analysis of $L^2(R)$ is defined as a sequence of closed subspaces V_j of $L^2(R)$, $j \in Z$, with the following properties:

- $V_j \subset V_{j+1}$
- $v(x) \in V_j \Leftrightarrow v(2x) \in V_{j+1}$
- $v(x) \in V_0 \Leftrightarrow v(x+1) \in V_0$
- $\bigcup_{j=-\infty}^{+\infty} V_j$ is dense in $L^2(R)$ and $\bigcap_{j=-\infty}^{+\infty} V_j = \{0\}$
- A scaling function $\varphi \in V_o$, with a non-vanishing integral, exists such that the collection $\{\varphi\{x \Leftrightarrow l) \big| l \in Z\}$, is a Riesz basis of V_o

A signal can be successively approximated by wavelets with different scales (multiresolution decomposition). Each step of the decomposition of signal corresponds to a certain resolution. The decomposition process can be iterated, with successive approximations being decomposed in turn, so that one signal is broken down into many lower-resolution components. This is called the wavelet decomposition tree. For n-level decomposition, there are n+1 possible ways to decompose or encode the signal.

The *wavelet packet transform (WPT)* method is a generalization of wavelet decomposition. In wavelet packet transform, the details as well as the approximations can be split. This yields more than 2^{2n-1} different ways to encode the signal. Wavelet packet decomposition is depicted in figure 4 (a).

Let $\phi(t)$ and $\psi(t)$ be the scaling function and the corresponding mother wavelet function in the conventional DWT and define $\psi^o(t) = \phi(t)$, and $\psi^1(t) = \psi(t)$, For 2^N sampled waveform the wavelet transform coefficients (WTCs) of a given function B(t) at the j level and k^{th} point can be evaluated by convolving the sequence $d^i_{j-1}(k)$ with a low pass filter (LPF), and then downsampling by a factor of two. In the same manner, coefficients (WTCs) of a given function B(t) at the $(2i+1)^{th}$ node can be evaluated by convolving the sequence $d^i_{j-1}(k)$ with a High pass filter (HPF), and then downsampling by a factor of two. Number of bands at j^{th} level is 2^j. Mathematically, the (WTCs) can be written as:

$$d_j^{2i}(k) = \int B(t)\psi_{j,k}^{2i}(t)dt = \sum_n h(n)d_{j-1}^i(2k-n)$$
$$d_j^{2i+1}(k) = \int B(t)\psi_{j,k}^{2i+1}(t)dt = \sum_n g(n)d_{j-1}^i(2k-n) \quad (2)$$

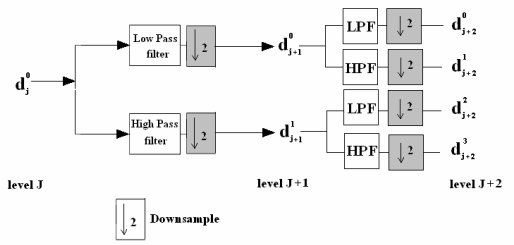

(a)

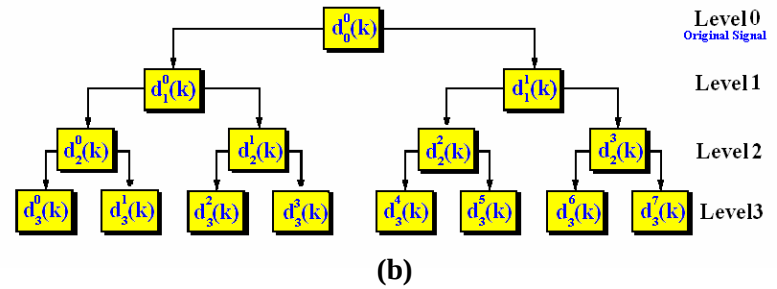

(b)

Figure 5(a): Wavelet Packet decomposition with successive filtering and down sampling. (b) Three level wavelet Packet decomposition

Where,

$$\psi_{j,k}^{2i}(t) = \frac{1}{\sqrt{2^j}}\psi^{2i}\left(\frac{2^j k - t}{2^j}\right) = \sum_n h(n)\psi_{j-1,2k-n}^{i}(t)$$

$$\psi_{j,k}^{2i+1}(t) = \frac{1}{\sqrt{2^j}}\psi^{2i+1}\left(\frac{2^j k - t}{2^j}\right) = \sum_n g(n)\psi_{j-1,2k-n}^{i}(t)$$

They are the wavelet basis function

j=0,1,….,N

i = 0, 1,……, $2^{j-1}-1$

Since the wavelet basis is orthogonal, the following properties should be fulfilled:

$$\int \psi_{j,k}^{P}(t)dt = 0 \qquad \text{p=integer}$$

$$\int \psi_{j,k}^{P}(t)\psi_{j,k}^{q}(t) = \begin{cases} 1 & \text{p=q} \\ 0 & p \neq q \end{cases} \qquad (3)$$

$$\int (\phi_{j,k}(t))^2 = 1$$

$$\int \phi_{j,k}(t)\psi_{j,k}^{p}(t) = 0 \qquad \text{p} \neq 0$$

A three level wavelet packet decomposition tree is shown in figure 4b. Each tree represents the signal decomposition as depicted in figure 4a.

5. Wavelet representation of RMS and total harmonic distortion

In the wavelet theory, any waveform can be expressed in terms of it's weighted sums of wavelet basis function, hence B(t) can be expressed as:

$$B(t)=\sum_{i=0}^{2^{j-1}-1}\sum_{k=0}^{2^{N-J}-1} d_j^{2i}(k)\psi_{j,k}^{2i}(t)+\sum_{i=0}^{2^{j-1}-1}\sum_{k=0}^{2^{N-J}-1} d_j^{2i+1}(k)\psi_{j,k}^{2i+1}(t)=\sum_{k=0}^{2^{N-J}-1} d_j^{0}(k)\phi_{j,k}(t)+\sum_{i=1}^{2^{j-1}-1}\sum_{k=0}^{2^{N-J}-1} d_j^{i}(k)\psi_{j,k}^{i}(t) \quad (4)$$

Where $d_j^0(k)$ is the scaling function coefficients .

RMS of a waveform with period T can be expressed in terms of wavelet at a certain level j as follows:

$$\int B(t)^2 dt=\int[\sum_{k=0}^{2^{N-J}-1} d_j^{0}(k)\phi_{j,k}(t)+\sum_{i=1}^{2^{j-1}-1}\sum_{k=0}^{2^{N-J}-1} d_j^{i}(k)\psi_{j,k}^{i}(t)]^2 dt=\int[\sum_{k=0}^{2^{N-J}-1} d_j^{0}(k)\phi_{j,k}(t)]^2 dt+\int[\sum_{i=1}^{2^{j-1}-1}\sum_{k=0}^{2^{N-J}-1} d_j^{i}(k)\psi_{j,k}^{i}(t)]^2 dt]^2$$

$$+2\int\left(\sum_{i=1}^{2^{j-1}-1}\sum_{k=0}^{2^{N-J}-1} d_j^{0}(k)d_j^{i}(k)\phi_{j,k}(t)\psi_{j,k}^{i}(t)\right)$$

$$=[\sum_{k=0}^{2^{N-J}-1}(d_j^{0}(k))^2\int[\phi_{j,k}(t)]^2 dt+\sum_{i=1}^{2^{j-1}-1}\sum_{k=0}^{2^{N-J}-1}(d_j^{i}(k))^2\int[\psi_{j,k}^{i}(t)]^2 dt+2\left(\sum_{i=1}^{2^{j-1}-1}\sum_{k=0}^{2^{N-J}-1} d_j^{0}(k)d_j^{i}(k)\int\phi_{j,k}(t)\psi_{j,k}^{i}(t)dt\right) \quad (5)$$

Using the wavelet orthogonality property, (5) becomes:

$$\int \mathrm{B(t)}^2 dt=\sum_{i=0}^{2^{j}-1}\sum_{k=0}^{2^{N-j}-1}(d_j^{i}(k))^2 \quad (6)$$

The RMS of the flux waveform can now found by divided by the wave period T and take the root square of (6).

$$B_{rms}=\sqrt{\frac{1}{T}\int_0^T B(t)^2}=\sqrt{\frac{1}{2^N}\sum_{n=0}^{2^N-1}B(n)^2}=\sqrt{\frac{1}{2^N}\sum_{n=0}^{2^{j}-1}\sum_{k=0}^{2^{N-j}-1}(d_j^{i}(k))^2}=\sqrt{\sum_{n=0}^{2^{j}-1}(B_j^{i})^2} \quad (7)$$

$$B_j^{i}=\sqrt{\frac{1}{2^N}\sum_{k=0}^{2^{N-j}-1}(d_j^{i}(k))^2} \quad (8)$$

Where, B_j^i is the RMS value of frequency band at node i. The Total Harmonic band distortion (THBD) is defined by the ratio of the RMS value of the harmonic bands at i >0 (i.e. excluding the lowest band) to the RMS value of the distorted waveform. The THBD for the flux density waveform is given by the following relation:

$$\mathrm{THBD}=\frac{1}{B_{rms}}\sqrt{\sum_{i=1}^{2^{j}-1}(B_j^{i})^2} \quad (9)$$

6. Results and discussion

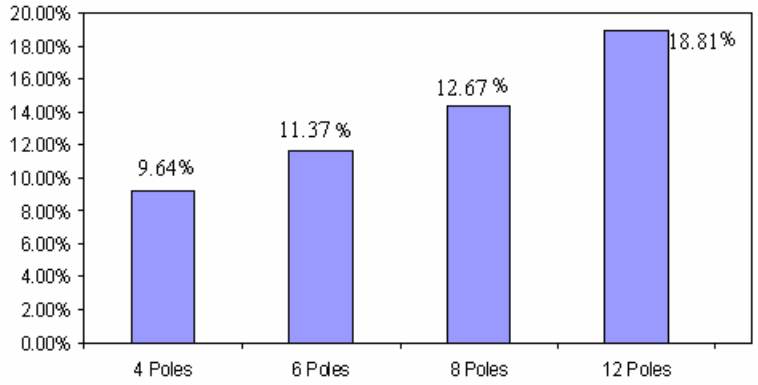

Figure 6: THBD change with number of poles change

Table 1:Total harmonic distortion for different number of poles in case of original rotor pole structure

	THD %	RMS	Band 0 0-75Hz	Band 1 75-150Hz	Band 2 150-225Hz	Band 3 225-300Hz	Band 4 300-375Hz
4 poles	9.64	0.635	0.632	0.0304	0.0261	0.0146	0.0123
6 poles	11.37	0.6066	0.6027	0.056	0.0276	0.016	0.0137
8 poles	12.67	0.6163	0.6113	0.0635	0.0347	0.0177	0.0172
12 poles	18.81	0.5713	0.5611	0.091	0.0444	0.0194	0.0232

Table 2:Total harmonic distortion for different number of poles in case of smooth rotor pole structure

	THD %	RMS	Band 0 0-75Hz	Band 1 75-150Hz	Band 2 150-225Hz	Band 3 225-300Hz	Band 4 300-375Hz
4 poles	9.2	0.5737	0.5713	0.0432	0.0212	0.0145	0.0103
6 poles	11.63	0.5913	0.5873	0.0576	0.0280	0.0153	0.0137
8 poles	14.4	0.5824	0.5766	0.0695	0.0331	0.0144	0.0168
12 poles	18.95	0.5600	0.5498	0.0907	0.0446	0.0166	0.0219

Wavelet Packet technique has been applied to the flux density in the middle of the air gap obtained from the finite element model to extract the different harmonic bands of the flux density waveform. A five level decomposition was selected to perform our study. This will decompose the signal into 32 frequency band (2^5). The first eight are enough to evaluate the harmonic behaviors. From the analysis it is clear that there is increase in harmonics contents within the flux density with the number of poles increase. Figure 6 shows the relation between number of poles increase and the total harmonic band distortion. There is a small increase in the THBD from 4 to 6 poles machine. On the other hand bigger increase is noticed between 6 and 8 poles, 6 and 12 poles, and 8 and 12 poles respectively. Table 1 shows the analysis result of the flux waveform for the first 4 frequency band for 4, 6, 8 and 12 poles of PM original structure rotor respectively. Table 2 shows similar results for smooth rotor structure design motor. Details and results about designing this smooth rotor can be found in [Mohammed et al., 2004]. If we compare corresponding values for each pole, there is only minimal change in the total harmonic band distortion. Results show that changing the rotor structure from protruding shape to smooth rotor does not change the harmonic contents appreciably in the air gap flux density waveform.

7. Conclusion

Finite element simulation presents an effective method for studying the influence of internal structure changes on the harmonic content of the working flux density. A wavelet packets technique was used to evaluate the harmonic behavior for different number of poles. The property of WPT analysis shows an ability to quantify different types of signals. It also shows high ability of wavelets to extract the different harmonic components disregarding the length of their occurrence in time. The harmonic contents tend to increase with number of poles increase but do not change with the changes in the rotor structure design significantly. The results are very useful in the design and development of both the motor and drive's diagnosis systems**.**

8. References

Angrisani L, Daponte P, D'Apuzzo M, and Testa A, "A measurement method based on the wavelet transform for power quality analysis," IEEE Transactions on Power Delivery, Vol.13, No. 4, Oct. 1998

Elliott D, "Handbook of digital signal processing: engineering applications," Academic Press, INC, 1987

Galli A. W, "Analysis of electrical transients in power systems via a novel wavelet recursion method," Purdue University, 1997

Goswami J. C., and Chen A .K , "Fundamentals of wavelets," John Wiley, 1999

Hamid E, Kawasaki Z, Yoshida H, and Doi H, "Wavelet analysis of voltage disturbances for power quality applications," IEE of Japan, Vol.122, No.2, February 2002

Kaiser Gerald, "A friendly guide to wavelets," Springer Verlag, 1994

Mao P.L, and Aggarwal R.K, "A novel approach to the classification of the transient phenomena in power transformers using combined wavelet transform and neural network," IEEE Transactions on Power Delivery, Vol. 16, No. 4, Oct. 2001

Madisetti V. K., and Williams D. B., "Digital signal processing handbook," CRC Press, 1999

Mohammed O.A., Abed N., Ganu S. and Liu S., "Wavelet analysis of permanent magnet synchronous machine flux density harmonic content with different pole number designs," ACES 2004

Press W et al., "Numerical recipes in fortran," Cambridge University Press, New York, 1992

Wang Fan, "On power quality and protection," Thesis, Chalmers University of Technology, 2000

Wornell G, "Signal processing with fractals: A wavelet-based Approach," Prentice Hall, 1996

Yoon W and Devancy M, "Power measurement using the wavelet transform," IEEE Transactions on Instrumentation and Measurements, Vol. 47, No.5, OCT 1998